Ultrasonics 133 (2023) 107047

Contents lists available at ScienceDirect

Ultrasonics

journal homepage: www.elsevier.com/locate/ultras

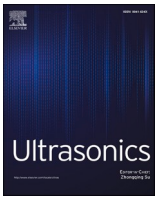

Short communication

Guided wave skew velocity correction in anisotropic laminates

F. Hervin *, P. Fromme

Department of Mechanical Engineering, University College London (UCL), UK

ARTICLE INFO

Keywords:
Lamb Waves
Composites
Anisotropy
Beam steering
CFRP

ABSTRACT

Guided ultrasonic wave propagation in anisotropic structures results in directional dependency of velocity and wave skewing effects that can impact the accuracy of damage detection. Phase and group velocities of the A_0 guided wave mode, propagating in a unidirectional carbon fiber reinforced laminate, were investigated experimentally and through finite element analysis. A correction for the significant offset in phase and group velocities due to wave skewing effects is illustrated for both point and short line sources, achieving good agreement with theoretical calculations assuming planar wave fronts. The influence of the line excitation length on velocity measurements is discussed.

1. Introduction

Guided wave based structural health monitoring (SHM) of fiber reinforced composite aircraft components is a promising technique to detect barely visible impact damage (BVID) caused by low velocity impacts [1,2]. However, guided wave propagation in composites is complex and influenced by the anisotropic material properties [3], in addition to the environmental and operational conditions [4]. In particular, material anisotropy of fiber reinforced laminates causes a number of wave propagation effects such as directional dependency of wave velocities [5] and amplitudes [6,7], in addition to wave steering [8] and beam spreading [9]. Left unaccounted for, this could lead to errors in damage localization. With many SHM techniques dependent on time-of-flight methods [10], accurate measurement of guided wave velocities is required.

Guided wave theory assumes (infinite) plane wave fronts launched in a given direction relative to the material anisotropy orientation (e.g., fiber direction) [11]. This cannot be replicated exactly in 3D Finite Element (FE) simulations and experiments, where line sources of finite length or point sources for selective excitation of guided wave modes are employed, e.g., piezoelectric discs. Measurements should be conducted in the far field (several wavelengths), where the curved wavefront from the point source approximates the theoretically assumed planar wavefront. For isotropic (e.g., aluminum) plates, good agreement of experimentally measured phase and group velocities from a point source with theoretical calculations has been widely reported in literature [12,13]. In anisotropic plates, wave energy tends to be focused towards the high stiffness fiber directions. The energy of the wave packet is steered along the group direction, but the wavefronts remain perpendicular to the wave launching (phase) direction [11]. The amount of steering is defined by the wave skew angle, the difference between the phase (wave launching) and group (wave propagation) directions. Severe skew angles have been observed in composites [14,15]. Several studies have considered the wave steering [8,16–19] and energy focusing effects in composites [3,20].

Guided wave velocities in anisotropic materials are directionally dependent, with the material anisotropy leading to higher velocities in the high stiffness (fiber) directions. As individual mode velocities are also frequency dependent, this results in three-dimensional dispersion curves [17], making damage detection more complex than for isotropic structures. In unidirectional carbon fiber reinforced plastics (CFRP), the velocity of the fundamental symmetric guided wave mode (S_0) is highly directionally dependent. The A_0 mode (fundamental anti-symmetric mode) has lower directional variation, although still significant enough to impact damage detection [6]. The directional dependency of wave velocities in anisotropic materials has been well established. Putkis et al measured strong directional dependency of energy velocity for the S_0, SH_0, and A_0 modes in a unidirectional CFRP plate and ensured measurements were performed along the energy direction to minimize skew effects [21]. De Luca et al considered the directional dependency of group velocity of the A_0 and S_0 modes in flat and curved plates at a range of excitation frequencies [22]. Measured A_0 and S_0 mode phase velocities in silicon wafers, an orthotropic material with similar anisotropy and steering behavior to CFRP, were lower than predicted by theory in the non-principal directions [18]. Zhao et al demonstrated that the propagation directions of phase and group velocity do not align in

* Corresponding author.
E-mail address: flora.hervin.19@ucl.ac.uk (F. Hervin).

https://doi.org/10.1016/j.ultras.2023.107047
Received 14 November 2022; Received in revised form 15 March 2023; Accepted 14 May 2023
Available online 18 May 2023

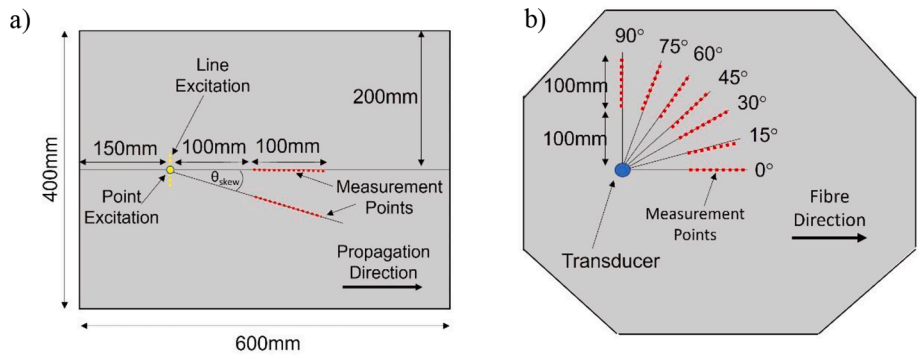

Fig. 1. a) Geometry of FE model showing excitation and monitoring locations; b) schematic of transducer and measurement locations for experimental measurements.

the same direction in anisotropic plates and so the phase velocity should be transformed into the group direction based on the skew angle [23]. Rhee et al proposed a magnitude and direction correction for the theoretical S_0 mode group velocities in composite plates [24]. Wang and Yuan calculated group velocities from 3D elasticity theory for comparison to experimental results [25]. Whilst numerous studies have considered the effect of anisotropy on group velocity, the experimental measurement of the directional dependence of phase velocity has not been widely reported and compared to theoretical predictions.

In this contribution phase and group velocities of point and line A_0 mode sources were calculated from FE models of a unidirectional CFRP panel. The FE model was validated by non-contact laser measurements and compared to theoretical values from dispersion curves. A significant offset in raw phase and group velocities was observed for both a point and a short line source. Wave skew behavior is discussed, and a velocity correction based on the skew angle is illustrated and applied to the measured and simulated velocities, achieving good agreement with theory. The validity of the correction over a range of frequencies is established and the influence of excitation length discussed.

2. Finite element modelling and experimental measurements

Full 3D FE simulations of a unidirectional CFRP plate section with dimensions 600 mm × 400 mm × 3.6 mm were carried out in ABAQUS/Explicit. A model input file, specifying parameters and geometry, was generated in MATLAB before being imported into ABAQUS 2018 for analysis. The plate was modelled as an anisotropic, homogenized structure. Previously measured material properties of the CFRP laminate were used [26]. Eight node solid brick elements (C3D8R) were selected for the model with an element size of 0.5 mm × 0.5 mm × 0.45 mm (eight elements through the plate thickness) and the time increment and simulation time were set to 5 ns and 150 μs respectively, fulfilling the usual stability criteria. The stiffness proportional Rayleigh damping coefficient was set to $\beta = 70$ ns. Point source excitation of the A_0 mode was implemented by applying an out-of-plane force to a single node. The narrowband excitation pulse was a 100 kHz, 5 cycle sine wave modified by a Hanning window. At this frequency the A_0 mode has a wavelength (λ) of approximately 16 mm in the 0° direction. A line excitation was generated by applying simultaneous out-of-plane forces along a line of nodes, 40 mm and 80 mm in length.

History outputs for the out-of-plane displacements were requested along a 100 mm line of monitoring points, originating 100 mm from the excitation with a step size of 1 mm, as shown in Fig. 1. In order to model wave propagation in different incident wave directions, the orientation of the material properties was rotated whilst keeping the model geometry and monitoring locations the same. Material properties were rotated in 5° steps between 0° and 90°. A separate simulation was performed in each direction for each excitation type. Additionally, for the 40 mm line excitation, a 100 mm line of measurement points, oriented along the skew angle of the corresponding material property orientation was defined as shown in Fig. 1a.

Guided wave measurements were performed on an undamaged 24-ply unidirectional CFRP specimen (dimensions 1.14 m x 0.94 m with corners removed) with 3.6 mm thickness (ply thickness 0.15 mm). A piezoceramic transducer (lead zirconate titanate (PZT), Ferroperm Pz27, diameter 5 mm, thickness 2 mm) with a brass backing mass (diameter 5 mm, thickness 6 mm) was bonded to the plate surface and used for the point source excitation of the A_0 mode. An excitation signal of a 100 kHz, 5 cycle sine wave modulated by a Hanning window was generated by a programmable function generator. The excitation signal was amplified to 100 Vpp before being applied to the transducer. A laser vibrometer attached to a scanning rig was used to measure the velocity

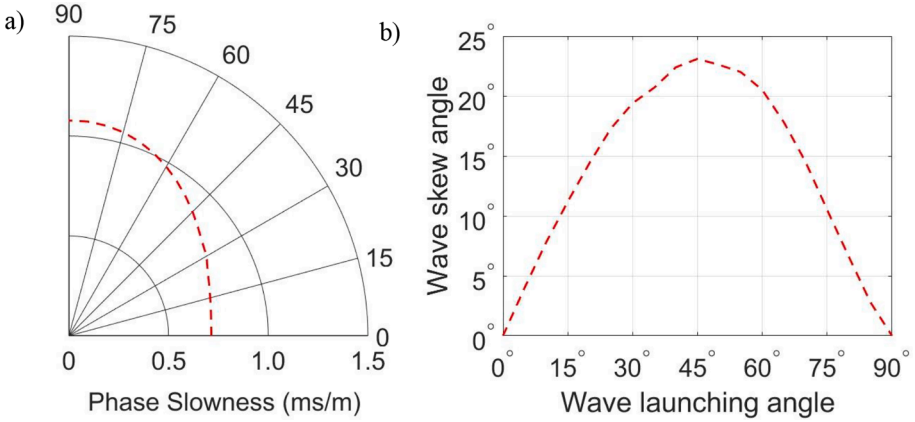

Fig. 2. a) Phase slowness curve for A_0 mode at 100 kHz in 3.6 mm thick unidirectional CFRP; b) theoretical skew angle with respect to wave launching direction.

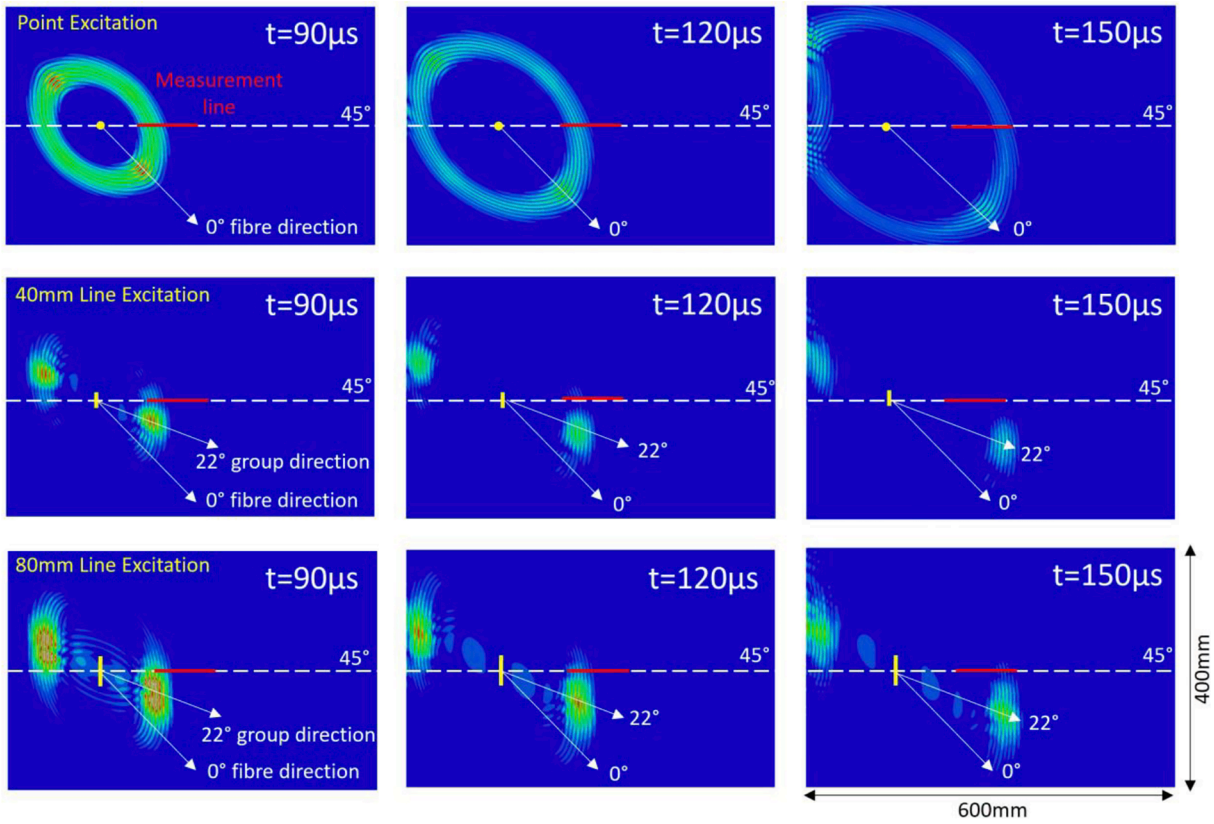

Fig. 3. Normalized displacement magnitude contour plots for different source types in 45° wave launching direction. Obtained from FE simulations at time snapshots 90 ns, 120 ns, 150 ns, respectively. Top row: point source; middle row: 40 mm line source; bottom row: 80 mm line source.

of the out-of-plane displacement at the plate surface. Retro-reflective tape was applied to the surface of the plate to improve laser beam reflection and subsequently the signal to noise ratio. Time signals were filtered using a band pass filter with cut-off frequencies of 75 kHz and 125 kHz, respectively. Radial lines, 100 mm length in 1 mm steps, were scanned every 15° at a distance of 100 mm from the transducer, shown schematically in Fig. 1b.

3. Results and discussion

3.1. Wave skew effects

Theoretical group and phase velocity dispersion curves for the A_0 mode in a 3.6 mm thickness unidirectional CFRP laminate were obtained using the Disperse software with the same material properties as used for the FE simulations [26]. Individual dispersion curves were calculated for each wave launching direction between 0° and 90° in 5° increments relative to the fiber orientation. The theoretical phase slowness curve was calculated by taking the inverse of phase velocity of the A_0 mode at 100 kHz for each wave launching angle as shown in

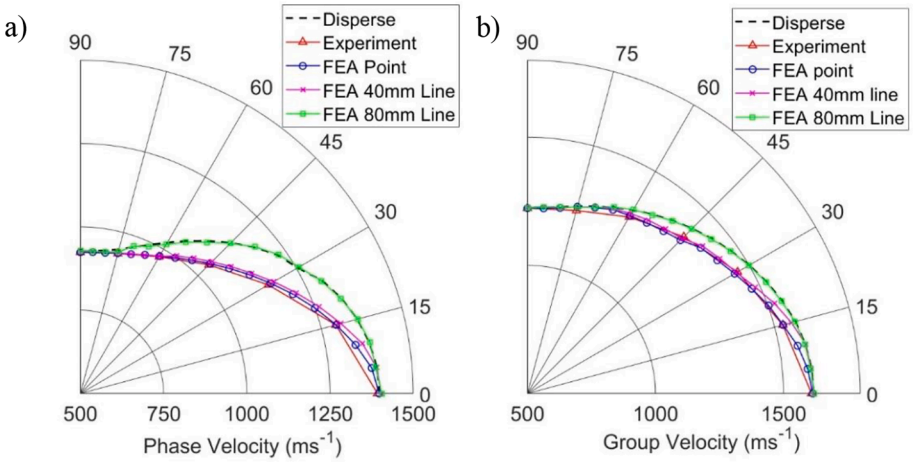

Fig. 4. Raw, uncorrected measured and simulated a) phase and b) group velocities of the A_0 mode at 100 kHz for a point, 40 mm line, and 80 mm line source respectively, compared to theory (Disperse).

Fig. 2a. The group direction at a particular wave launching (phase) angle can be obtained by calculating the normal to the tangent of the slowness curve. The theoretical wave skew angle is obtained as the difference between the phase and group directions and is plotted for each incident wave direction in Fig. 2b. Zero skew angle is observed along the principal (0° and 90°) directions. The highest skew angle of 23° is predicted in the 45° direction.

Time snapshots of the out-of-plane displacement for point, 40 mm line, and 80 mm line sources are presented in Fig. 3 for the 45° wave launching direction. The 45° direction is aligned along the dashed white lines. For the point source (top row Fig. 3) an oval shaped wavefield can be observed due to the anisotropy influencing waves directed radially outwards from the source. Higher amplitude and wave velocity along the 0° direction can be observed, indicating that energy focusing is occurring along the fibers as expected. For the 40 mm line excitation, the finite width of the excitation can be clearly observed. Despite significant wave steering the wavefronts remain parallel to the wave launching direction. However, the wave pulse has been significantly steered away from the wave launching direction. For the 80 mm line source the wavefronts also remain parallel to the wave launching direction. Wave steering again is observed, however the pulse has sufficient length for a measurement line in the original wave launching direction to capture some of the energy of the pulse.

3.2. Uncorrected velocity values

Phase and group velocities were calculated for each excitation type and each wave launching direction. The phase velocity was calculated by taking the FFT of each signal plotting the phase angle at the center frequency f (100 kHz) against distance from the source, taking care to remove any 2π phase jumps. A linear fit was performed, and the gradient of the line extracted. Multiplying the inverse of this gradient by a factor of $2\pi f$ yields the phase velocity. Additionally, the arrival time of the maximum of the Hilbert envelope of the time signal was plotted against distance from the source for each measurement point in a given direction. A linear fit was then performed, and the gradient of the line extracted. The group velocity is equal to the inverse of this gradient. Fig. 4a shows the raw experimental and FE phase velocity and group velocity measured for different wave launching directions, compared to theoretical values from Disperse. Good agreement is observed between the point source FE and the experimental measurements from a PZT disc, indicating that the FE accurately captures wave propagation behavior occurring in the physical specimen. The velocities along the principal axes (0° and 90° zero skew angle) are in good agreement (1%) with the theoretical values. However, a significant offset between theory and measurement can be observed in the non-principal directions with the largest discrepancy (8%) observed in the 45° direction (highest predicted wave skew angle of 23°, see Fig. 2b). The offset is most likely caused by wave steering effects due to anisotropy not being accurately accounted for. Similar behavior can be observed for the group velocities in Fig. 4b.

The velocities from the 40 mm (~2λ) line source have similar values to those of the point source. As the length of the source is increased to 80 mm (~5λ), the phase and group velocities match the theoretical predictions within 1%. It was initially thought that the offset was related to the ratio of the length of the line source to the wavelength, with a longer line source behaving more similarly to a planar wavefront, originating from Huygens principle where a planar wavefront can be considered as an infinite line of point sources [27]. However, the offset is caused by wave skewing effects. As seen in Fig. 4, the magnitude of the error for the point and 40 mm line source from the theoretical values is related to the magnitude of the skew angle in that direction (shown in Fig. 2b), i.e., a larger skew angle results in a larger offset from theory. As seen in the time snapshots in Fig. 3, the 40 mm (~2λ) line source generates a directional pulse with reasonably planar wavefronts. However, for the 45° wave launching direction with significant steering angle (23°) limited pulse amplitude is detected along the perpendicular measurement line. Conversely, the 80 mm line source gives a similar directional pulse but the planar wavefronts are long enough for the perpendicular measurement lines to capture sufficient pulse energy despite the significant steering, resulting in more accurate phase and group velocities. Care needs to be taken to monitor in directions where pulse energy is travelling due to the anisotropy effects so that accurate velocity measurements can be obtained.

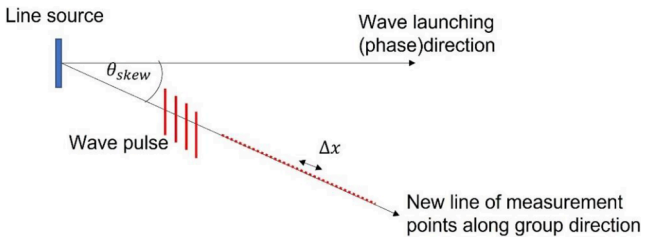

Fig. 5. Schematic of skew angle corrections for a linear source.

The results (Fig. 4) indicate that wave steering effects impact the accuracy of velocity measurements, with significant offsets observed for both the point and 40 mm line source. A skew angle correction should therefore be applied to the phase and group velocities to mitigate this offset.

3.3. Corrected velocity values

To accurately measure velocities from the 40 mm FE line source, a diagonal line of measurement points (as shown in Fig. 1a) was defined along the group direction (obtained from Fig. 3a) as shown in Fig. 5. This enables the velocity measurement to be taken in a region where sufficient wave energy is present. As the wave fronts stay parallel to the wave launching direction, a projection of the phase or group velocity can then be calculated along the wave launching (phase) direction by multiplying the uncorrected phase or group velocity by a factor of $\cos(\theta_{skew})$, where θ_{skew} is the wave skew angle. For the point source, measuring a region of the wavefront with sufficient energy is less of an issue (see Fig. 3), but wave skewing effects occur. In this case the wave pulse measured in a given direction will have actually originated at a different phase direction and steered due to anisotropy. To calculate the corrected velocity, the velocity along the corresponding group direction should be projected into the wave launching (phase) direction by multiplying by a factor of $\cos(\theta_{skew})$. For example, waves launched in the 45° direction have a skew angle of 23°, so taking the velocity in the 22° direction (group direction) and multiplying by cos(23°) will yield the correct velocity value. The uncorrected velocities shown in Fig. 4 were obtained in 5° increments, so velocity values were interpolated to obtain uncorrected values in 1° increments.

The corrections described above were applied to the velocity values shown in Fig. 4. Corrected phase and group velocity values for a point and 40 mm line source are shown in Fig. 6. Good agreement (within 1%) between the measured, simulated, and theoretical values can be observed, which indicates that the applied correction is appropriate, and that the offset observed in Fig. 4 is caused by wave skew effects. However, it should be noted that either reasonable estimates for the phase velocity dispersion curves, and therefore the material properties, are required or wave skew angles need to be measured. These results indicate that, provided wave skew effects are considered, guided waves generated from a point source can accurately match theoretical predictions in strongly anisotropic media. This is advantageous as a point source is significantly easier to implement experimentally than the longer line sources investigated in the FE simulations.

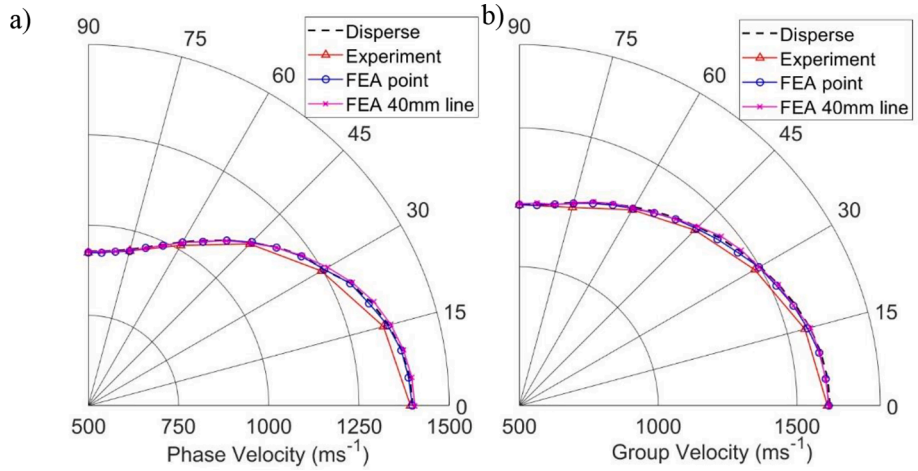

Fig. 6. Measured and simulated a) phase and b) group velocities of the A_0 mode at 100 kHz for different source types with skew angle correction applied.

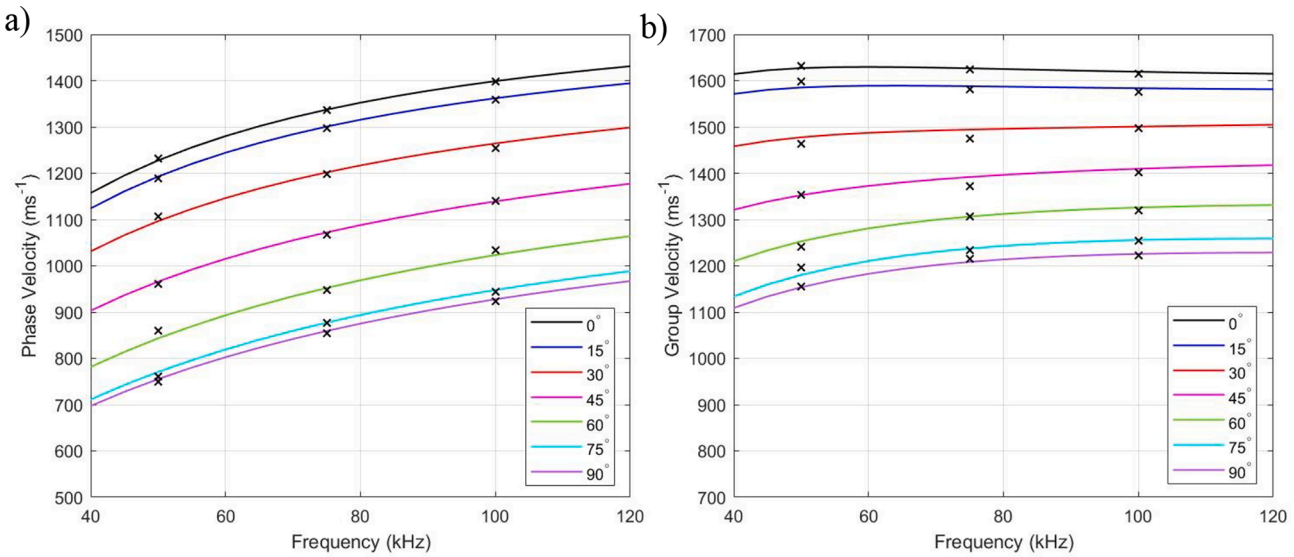

Fig. 7. a) Phase and b) group velocity dispersion curves for the A_0 mode in 3.6 mm thick UD CFRP for wave launching directions 0°-90° (relative to fiber direction), obtained from Disperse software. Black crosses show corrected FE point source values at 50 kHz, 75 kHz, and 100 kHz.

3.4. *Influence of excitation frequency*

The above presented results were for a center frequency of 100 kHz. Fig. 7 shows the phase and group velocity dispersion curves for the A_0 mode in a range of wave launching angles. A frequency range of 40–120 kHz is considered. Below this range the A_0 mode experiences significant dispersion and at higher frequencies the attenuation of the A_0 mode significantly reduces propagation distance, making guided wave measurements impractical. The validity of the velocity correction was additionally investigated at 50 kHz and 75 kHz. At the lower frequencies a greater offset (12%) from the theoretical values was found in the high skew directions as the maximum skew angle also increased (25° at 75 kHz, 28° at 50 kHz), but this was adequately compensated for by the skew angle correction (see Appendix). The corrected FE point source velocity values for various frequencies are denoted by the black crosses in Fig. 7, showing good agreement with theoretical values.

Wave skew angle and the velocity correction should be considered when there is a significant directional variation in velocity and significant skew angles that could lead to errors in damage localization, particularly when considering SHM methods that rely on velocity measurements. Care should be taken when using PZT disc transducers, which behave similarly to the point sources considered here. The unidirectional laminate considered in this study shows more severe wave skewing behavior than cross-ply and quasi-isotropic layups. However, it has been demonstrated that anisotropic effects can still be significant for quasi-isotropic layups [5], therefore care should be taken when considering wave propagation in anisotropic composite structures.

4. Conclusions

Phase and group velocities of the A_0 mode in a highly anisotropic unidirectional composite plate were investigated for point and line sources through finite element modelling and were compared to experimental measurements and theoretical predictions. Care should be taken when measuring velocities in an anisotropic material, particularly if using a point source such as a piezoelectric disc, as often selected for guided wave measurements, as velocities can be significantly under predicted in wave launching directions with high skew angles. It has been demonstrated that measured velocities can accurately match theoretical predictions either by using a line source of sufficient length to accurately capture pulse energy despite skewing, or by using a point or short line source but correcting for skew angle when calculating velocities. The validity of the velocity correction over a range of excitation

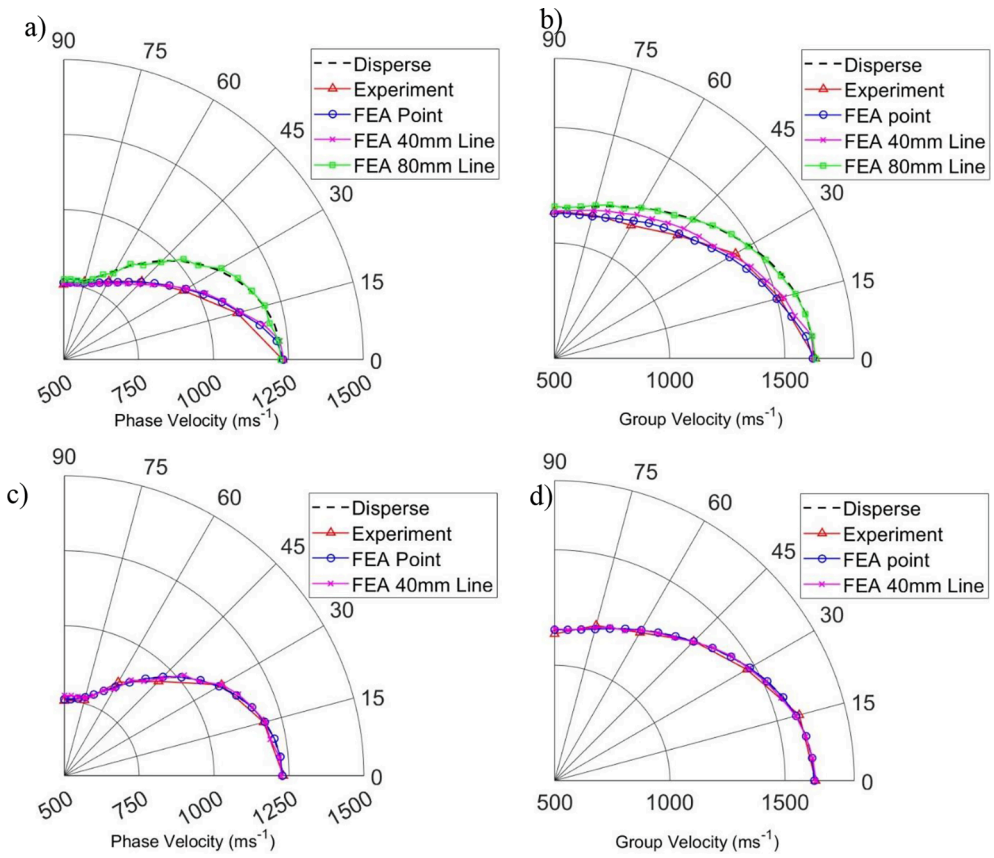

Fig. A.1. Measured and FEA simulation phase and group velocities of the A_0 mode at 50 kHz for different source types: a) phase velocity, uncorrected; b) group velocity uncorrected; c) phase velocity corrected; d) group velocity corrected.

frequencies has been established.

Declaration of Competing Interest

The authors declare that they have no known competing financial interests or personal relationships that could have appeared to influence the work reported in this paper.

Data availability

Data will be made available on request.

Appendix

Fig. A shows the uncorrected (Fig. A a/b) and corrected (Fig. A c/d) phase and group velocities for various source types at an excitation frequency of 50 kHz. As for the 100 kHz results in Fig. 4 and Fig. 6, the 80 mm line source velocities show good agreement with the theoretical values, without the need for a correction. For the point and 40 mm line sources, there is good agreement in the principal directions, but again a significant offset occurs in directions with high skew angle. The maximum offset from the theoretical values is 12% for the point source phase velocities at 45°. The appropriate velocity correction was applied to the point and 40 mm line source values, and as seen in Fig. A c/d, good agreement with theory is achieved.

References

[1] K. Diamanti, J.M. Hodgkinson, C. Soutis, Detection of low-velocity impact damage in composite plates using lamb waves, Struct. Health Monit. 3 (2004) 33–41.
[2] J.S. Hall, P. Fromme, J.E. Michaels, Guided wave damage characterization via minimum variance imaging with a distributed array of ultrasonic sensors, J. Nondestr. Eval. 33 (2014) 299–308.
[3] B. Chapuis, N. Terrien, D. Royer, Excitation and focusing of Lamb waves in a multilayered anisotropic plate, J. Acoust. Soc. Am. 127 (2010) 198–203.
[4] D. Perfetto, Z. Sharif Khodaei, A. de Luca, M.H. Aliabadi, F. Caputo, Experiments and modelling of ultrasonic waves in composite plates under varying temperature, Ultrasonics 126 (2022), 106820.
[5] G. Neau, M. Deschamps, M.J.S. Lowe, Group velocity of Lamb waves in anisotropic plates: Comparison between theory and experiments, AIP Conf. Proc. 557 (2001) 81–88.
[6] F. Hervin, P. Fromme, Anisotropy influence on guided wave scattering for composite structure monitoring, Struct. Health Monit. (available online 2022) . https://doi.org/10.1177/14759217221133284.
[7] W.K. Chiu, L.R.F. Rose, N. Nadarajah, Scattering of the Fundamental Anti-symmetric Lamb Wave by a Mid-plane Edge Delamination in a Fiber-composite Laminate, Procedia Eng. 188 (2017) 317–324.
[8] D. Chronopoulos, Wave steering effects in anisotropic composite structures: Direct calculation of the energy skew angle through a finite element scheme, Ultrasonics 73 (2017) 43–48.
[9] B.P. Newberry, R. B. Thompson, A paraxial theory for the propagation of ultrasonic beams in anisotropic solids, J. Acoust. Soc. Am. 85 (1989) 2290–2300.
[10] V. Memmolo, E. Monaco, N.D. Boffa, L. Maio, F. Ricci, Guided wave propagation and scattering for structural health monitoring of stiffened composites, Compos. Struct. 184 (2018) 568–580.
[11] E. Glushkov, N. Glushkova, A. Eremin, R. Lammering, Group velocity of cylindrical guided waves in anisotropic laminate composites, J. Acoust. Soc. Am. 135 (2014) 148–154.
[12] N. Hu, S. Takahito, F. Hisao, Z. Su, Damage identification of metallic structures using A0 mode of lamb waves, Struct. Health Monit. 7 (2008) 271–285.
[13] L. Yu, C.A.C. Leckey, Z. Tian, Study on crack scattering in aluminum plates with Lamb wave frequency-wavenumber analysis, Smart Mater. Struct. 22 (2013), 065019.
[14] H. Gao, Ultrasonic guided wave mechanics for composite material structural health monitoring, The Pennsylvania State University, 2007. PhD Thesis.
[15] F. Hervin, P. Fromme, Guided wave propagation and skew effects in anisotropic carbon fiber reinforced laminates, J. Acoust. Soc. Am. 153 (2023) 2049–2060.
[16] K.I. Salas, C.E.S. Cesnik, Guided wave structural health monitoring using CLoVER transducers in composite materials, Smart Mater. Struct. 19 (2010), 015014.
[17] M.J.S. Lowe, G. Neau, M. Deschamps, Properties of Guided Waves in Composite Plates, and Implications for NDE, AIP Conf. Proc. 700 (2004) 214–221.

[18] P. Fromme, M. Pizzolato, J. Robyr, B. Masserey, Lamb wave propagation in monocrystalline silicon wafers, J. Acoust. Soc. Am. 143 (2018) 287–295.
[19] F. Yan, J.L. Rose, Time delay comb transducers for aircraft inspection, The Aeronaut. J. 113 (2009) 417–427.
[20] C. Potel, S. Baly, J. de Belleval, M. Lowe, P. Gatignol, Deviation of a Monochromatic Lamb Wave Beam in Anisotropic Multilayered Media: Asymptotic Analysis, Numerical and Experimental Results, IEEE Trans. Ultrason. Ferroelectr. Freq. Control 52 (2005) 987–1001.
[21] O. Putkis, R.P. Dalton, A.J. Croxford, The anisotropic propagation of ultrasonic guided waves in composite materials and implications for practical applications, Ultrasonics 65 (2016) 390–399.
[22] A. de Luca, D. Perfetto, A. Polverino, A. Aversano, F. Caputo, Finite Element Modeling Approaches, Experimentally Assessed, for the Simulation of Guided Wave Propagation in Composites, Sustainability 14 (2022) 6924.
[23] J. Zhao, J. Qiu, H. Ji, Reconstruction of the nine stiffness coefficients of composites using a laser generation based imaging method, Compos. Sci. Technol. 126 (2016) 27–34.
[24] S.H. Rhee, J.K. Lee, J.J. Lee, The group velocity variation of Lamb wave in fiber reinforced composite plate, Ultrasonics 47 (2007) 55–63.
[25] L. Wang, F.G. Yuan, Group velocity and characteristic wave curves of Lamb waves in composites: Modeling and experiments, Compos. Sci. Technol. 67 (2007) 1370–1384.
[26] G. Neau, M.J.S. Lowe, M. Deschamps, Propagation of Lamb waves in anisotropic and absorbing plates: Theoretical derivation and experiments, AIP Conf. Proc. 615 (2002) 1062–1069.
[27] M. Born, E. Wolf, Principles of Optics, Cambridge University Press, 1999.